

Investigating the single production of vectorlike quarks decaying into a top quark and W boson through hadronic channels at the HL-LHC

A. C. Canbay^{✉*} and O. Cakir^{✉†}*Department of Physics, Ankara University, 06100 Ankara, Turkey* (Received 22 September 2023; accepted 5 October 2023; published 3 November 2023)

We investigate the single production of vectorlike quarks at the High Luminosity LHC (HL-LHC). With the assumed (enhanced) couplings to third generation quarks of the standard model, vectorlike quarks B/X are produced in association with a bottom (b) or top (t) quark, which correspond to Bbq and Btq/Xtq production modes, including an additional soft forward jet from the spectator quark (q). This study focuses on high-mass vectorlike quarks B/X decaying into a top quark and a W boson, resulting in the final state jets emerging from hadronically decaying top quark ($t \rightarrow Wb$) and W boson ($W \rightarrow q\bar{q}'$). The events with W boson and t quark have been analyzed using tagging techniques for large-radius jets. The scan ranges of the mass ($1000 < m_{B/X} < 3000$ GeV) for the relative width $\Gamma_{B/X}/m_{B/X} = 0.1$ and $\Gamma_{B/X}/m_{B/X} = 0.01$ of vectorlike B/X quarks have been investigated. From the results of the analysis, the masses of vectorlike quarks $B(X)$ up to 2491 (2364) GeV and 2018 (1873) GeV can be excluded corresponding to these relative width cases at 95% CL depending on the type and branching scenarios at integrated luminosity projection of 3 ab^{-1} at the HL-LHC.

DOI: [10.1103/PhysRevD.108.095006](https://doi.org/10.1103/PhysRevD.108.095006)

I. INTRODUCTION

The most of the phenomenological studies are focused on exploiting experimental data from the previous runs of particle colliders which provide the data corresponding to a luminosity delivered to particle detectors. A precise total cross section and differential cross section measurements of the single top quark production have been performed using data at $\sqrt{s} = 13$ TeV by the ATLAS and CMS Collaborations [1,2]. These studies aim also to pose constraints on theoretical models beyond the standard model (SM) of particle physics. These are also trying to predict the exclusion and/or discovery reaches of new searches during the next runs.

A variety of extensions of the SM predict the existence of new heavy particles. New heavy quarks (heavier than top quark) are generally expected to be of vectorlike nature if they exist. These particles could have a role in the stabilization of the Higgs boson mass, and hence promote a potential solution to the hierarchy problem. Vectorlike quarks (VLQs) are color triplets and their left-handed and right-handed components transform in the same way [3] under the electroweak symmetry group $SU(2)_L \times U(1)_Y$ of the SM.

In the predicting models, vectorlike quarks are expected to couple mostly to third generation quarks [4–6], and they can have both charged and neutral current interactions. A down type vectorlike B (VLB) quark with $-1/3$ can decay into Wt , Zb or Hb (their charge conjugation can also take place), while an up-type vectorlike T (VLT) quark can decay into Wb , Zt or Ht (and similarly their charge conjugation). The VLQs can arise in multiplets, such as singlets, doublets or triplets. In the minimal models, each scenario results in different T and B branching ratios. For singlets, the branching ratios are 50% for $B \rightarrow Wt$ and $T \rightarrow Wb$, and 25% for $B \rightarrow Hb/Zb$ and $T \rightarrow Ht/Zt$. A roadmap for the vectorlike singlet quark search has been reviewed theoretically and phenomenologically in Ref. [7]. However, in one of the doublet scenario the B decays only to Hb and Zb with equal branchings ratios of 50%, and similarly the T decays only to Ht and Zt with equal branchings, in another doublet scenario the B decays only to Wt , and similarly the T decays only to Wb with 100% branching ratio [5,6]. Experimental searches at the LHC mainly focused on singlets (T) and (B) with charges of $2/3$ and $-1/3$, respectively; or doublets (XT), (TB), and (BY) with the left and right chiralities for each of them. Here, vectorlike X (VLX) and Y (VLY) have their exotic charges of $5/3$ and $-4/3$, respectively. These can couple to the SM quarks through only charged currents, leading to decays $X \rightarrow Wt$ and $Y \rightarrow Wb$ with a branching ratio of 100%.

The model-independent pair production (via strong interaction) search results from the ATLAS and CMS collaborations, which set a limit on VLQ masses in the

* acanbay@cern.ch† ocakir@science.ankara.edu.tr

Published by the American Physical Society under the terms of the [Creative Commons Attribution 4.0 International license](https://creativecommons.org/licenses/by/4.0/). Further distribution of this work must maintain attribution to the author(s) and the published article's title, journal citation, and DOI. Funded by SCOAP³.

range of $O(1 \text{ TeV})$ independently of its electroweak representation. The single production of vectorlike quarks (via electroweak interactions) is affected by both the coupling strengths to the SM quarks and their masses, where a jet is emitted at a low angle to the beam direction. However, depending on multiplet structure, mass and coupling strength of VLQs the single production may overcome their pair production above few TeV range.

Previously, the ATLAS Collaboration have searched for the production of single vectorlike quarks in the Wt final state in pp collisions at $\sqrt{s} = 8 \text{ TeV}$ and set limits on the cross section of the single production of VLB quarks decaying into the Wt final state using a novel approach for boosted event topologies [8]. Searches performed recently by ATLAS and CMS Collaborations set limits on masses and couplings of different type of VLQs using proton-proton collision data at a center of mass energy of 13 TeV using Run 2 recorded data and simulated signal and background samples. The all hadronic final state is used for single vectorlike B quark production, and searched in CMS [9] in Hb intermediate states leading to three b -tag jets, two of them are reclustered in a Higgs-tag jet. The signature of the single production of VLB is used to categorize the signal region and separate it from the background. The search has used an integrated luminosity 35.9 fb^{-1} of data and set limits on the masses of 920 to 1490 GeV for vectorlike quarks B/X in the single lepton mode, at a relative width of 10% [10]. Recently, the search is carried out on 139 fb^{-1} of proton-proton collision data at $\sqrt{s} = 13 \text{ TeV}$ collected with the ATLAS detector between 2015 and 2018 runs. This search excludes the presence of a vectorlike B quark in the full hadronic mode with mass ranging between 1.0 TeV and 2.0 TeV for coupling $\kappa = 0.3$ [11]. Currently, some results are using the full Run 2 statistics, and more results are expected to provide the total available statistics very soon. In extension, the projections can be made for the High-Luminosity LHC (HL-LHC).

High energy particle collisions at the HL-LHC can lead to the production of massive particles (e.g. $W/Z/H$ bosons and top quarks) with much larger transverse momentum (p_T) than their rest mass. The decay products of such particles tend to be

collimated, or “boosted” along the direction of the parent particle. If the massive particles are sufficiently boosted, their overlapping hadronic decay products cannot be well reconstructed with small radius jets, and require large radius (large- R) jet reconstruction. The identification of hadronically boosted W boson decays with large- R jets is vital in many physics analyses at the LHC and HL-LHC. The dominant backgrounds are the jets originating from light quarks and gluons (QCD jets) as they occur at a much higher rate than boosted W -jets at high energy hadron collisions. Thus, boosted boson tagging and top tagging are used as the key techniques for searches of VLB/VLX in all hadronic decay mode, which also suppress the relevant background efficiently.

This paper is organized as follows: Section II describes the signal and background event generation and the simulation samples that are used in the physics analysis. We make estimations for the single production of vectorlike quarks at the HL-LHC at an integrated luminosity projection of 3 ab^{-1} . With the assumption of enhanced couplings to third generation quarks of the standard model, vectorlike B or X quark is produced in association with a bottom (b) or top (t) quark, which lead to Bbq and Btq/Xtq production modes, including an additional forward jet from the spectator quark (q). This study focuses on the intermediate state objects top quark and W boson (through $B \rightarrow Wt$ decay), and final state jets from hadronically decaying top quark ($t \rightarrow Wb$) and W boson ($W \rightarrow q\bar{q}'$). Section III describes the object definition, event selection, tagging and analysis of the simulated events. Section IV summarizes the reconstruction and statistical significance of VLB/VLX quark signal including the systematic uncertainties. Finally, in Sec. V, the conclusions have been drawn.

II. SIGNAL AND BACKGROUND EVENT GENERATION

The leading order representative Feynman diagrams of single production of VLB/VLX quark and decay chain are presented in Fig. 1. Note that the analysis has also included the charge-conjugate process. The VLB quark in this analysis is assumed to be in singlet or doublet representation, while

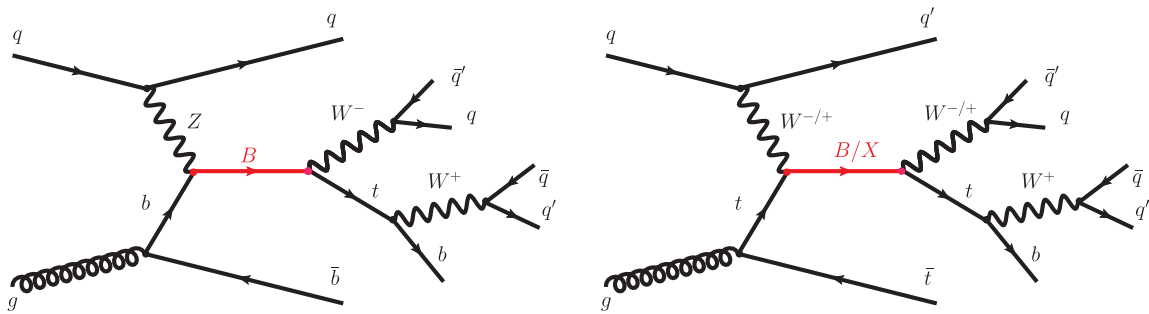


FIG. 1. Leading order representative diagrams for single production of vectorlike B quark [Z mediated (left) and of vectorlike B/X quark W mediated (right)] in association with a bottom quark (left) or top quark (right) and a light flavor quark, with the subsequent decays to a top quark and W boson leading to all hadronic mode.

TABLE I. Cross sections $\sigma(pp \rightarrow Bbj)$ and $\sigma(pp \rightarrow Btj/Xtj)$ (in pb) for Bbq and Btq/Xtq production process for different benchmark mass points considered in the analysis, where the couplings are calculated for a width to mass ratio of $\Gamma_{B/X}/M_{B/X} = 0.1$ with the branching ratios $\text{BR}(B \rightarrow Wt) = 0.5$, $\text{BR}(B \rightarrow Zb) = 0.25$ and $\text{BR}(B \rightarrow Hb) = 0.25$ corresponding to a singlet state. The numbers in the parenthesis correspond to Xtj production related to the coupling κ_W^X and branching ratio $\text{BR}(X \rightarrow Wt) = 1.0$. Cross section may depend on the chirality of the vector like quarks when different representation is considered.

Mass [GeV]	$\kappa_W^B (\kappa_W^X)$	κ_Z^B	κ_H^B	$\sigma(pp \rightarrow Bbj)$	$\sigma(pp \rightarrow Btj(Xtj))$
1000	0.4019(0.5683)	0.3840	1.6105	2.570×10^{-1}	$1.032 \times 10^{-1} (2.075 \times 10^{-1})$
1200	0.3302(0.4670)	0.3200	1.6027	9.837×10^{-2}	$4.028 \times 10^{-2} (8.107 \times 10^{-2})$
1400	0.2807(0.3969)	0.2743	1.5981	4.095×10^{-2}	$1.711 \times 10^{-2} (3.447 \times 10^{-2})$
1600	0.2442(0.3454)	0.2400	1.5951	1.866×10^{-2}	$7.940 \times 10^{-2} (1.596 \times 10^{-2})$
1800	0.2163(0.3059)	0.2133	1.5930	8.937×10^{-3}	$3.879 \times 10^{-3} (7.809 \times 10^{-3})$
2000	0.1942(0.2746)	0.1920	1.5916	4.440×10^{-3}	$1.962 \times 10^{-3} (3.952 \times 10^{-3})$
2200	0.1762(0.2491)	0.1745	1.5905	2.342×10^{-3}	$1.038 \times 10^{-3} (2.086 \times 10^{-3})$
2400	0.1612(0.2280)	0.1600	1.5897	1.248×10^{-3}	$5.541 \times 10^{-4} (1.116 \times 10^{-3})$
2600	0.1487(0.2102)	0.1477	1.5890	6.782×10^{-4}	$3.055 \times 10^{-4} (6.139 \times 10^{-4})$
2800	0.1379(0.1950)	0.1371	1.5885	3.790×10^{-4}	$1.700 \times 10^{-4} (3.426 \times 10^{-4})$
3000	0.1286(0.1819)	0.1280	1.5881	2.156×10^{-4}	$9.684 \times 10^{-5} (1.947 \times 10^{-4})$

the VLX quark is assumed to belong to a doublet. When the multiplet structure of vectorlike quarks is assumed, the possible final states and branching ratios require an approach involving simultaneous consideration of several final states [6]. The study reported here significantly extend the sensitivity to events in which a singly produced VLB/VLX quark decays to Wt followed by the hadronic decays $t \rightarrow Wb$ and $W \rightarrow jj$ in the resolved process. The use of fully hadronic decays allows the direct reconstruction of the VLB/VLX quark final state, and increases the expected signal-to-background ratio in the signal region defined for the search. Its sensitivity is considered to be studied by using tagging techniques resulting in a signal-to-background improvement.

This fully hadronic final state is of particular interest for vectorlike quark masses above 1 TeV. The resulting high- p_T jets from the top quark and W boson are “boosted,” so that the decay products of the top quark and W boson are collimated and captured in two large-radius (large-R) jets. This final state has the largest branching fraction of all the potential Wt decay modes and the large-R jets can be identified as either W -boson or top-quark candidates through tagging algorithms that use the substructure within the jet [12]. In addition, bottom-quark jet identification (b -tagging) provides background rejection with high efficiency given the bottom-quark jet coming from $t \rightarrow Wb$ decays. Assuming the existence of single VLB/VLX quark production within the narrow width approximation (NWA) for the parameter of relative decay width $\Gamma_{B/X}/m_{B/X} = 0.1-0.01$, the signal would appear as an excess of events with Wt invariant masses around the VLB/VLX quark mass.

The model framework for the VLQs has been used from the UFO format of VLQ model [13]. Signal and background events are generated using event generator MadGraph5_aMC-NLO [14] with the parton distribution function of NNPDF30 pdf set with *lhpdfid* 263400 [15],

and the parton showering and hadronization are performed with Pythia8 [16]. The signal cross sections for different production modes ($pp \rightarrow Bbq$, $pp \rightarrow Btq/Xtq$) are given in Table I. We have used all hadronic channels for each signal samples.

The cross sections of the relevant backgrounds and corresponding modes are given in Table II. For the benchmark mass values of 1500, 2000, and 2500 GeV, the couplings for the corresponding modes are calculated as $0.083:0.081:0.505$ for $\kappa_W:\kappa_Z:\kappa_H$ at a relative decay width of $\Gamma_B/m_B = 0.01$. A single decay mode for VLX lead to coupling values of $\kappa_W = 0.117, 0.087,$ and 0.069 for the same benchmark mass values at $\Gamma_X/m_X = 0.01$. We have generated events by using the SM-full model of MadGraph5_aMC-NLO [14] for top pair production, single top production and diboson production. We have also

TABLE II. The cross sections (in pb) of the relevant backgrounds and corresponding modes with the generated events (where k denotes thousand events units).

Background	Mode	Cross sections [pb]	Generated events [k]
$t\bar{t}$	$t\bar{t}$	5.990×10^2	179
	tj	7.394×10^{-1}	100
Single top	tb	8.655×10^0	100
	tW	2.553×10^{-1}	192
	WW	7.937×10^1	100
Diboson	WZ	3.021×10^1	100
	ZZ	1.156×10^1	100
$W + \text{jets}$ (matched)	$W + nj$ $n \leq 4$	2.674×10^5	64
	$Z + \text{jets}$ (matched)	$Z + nj$ $n \leq 4$	8.219×10^4

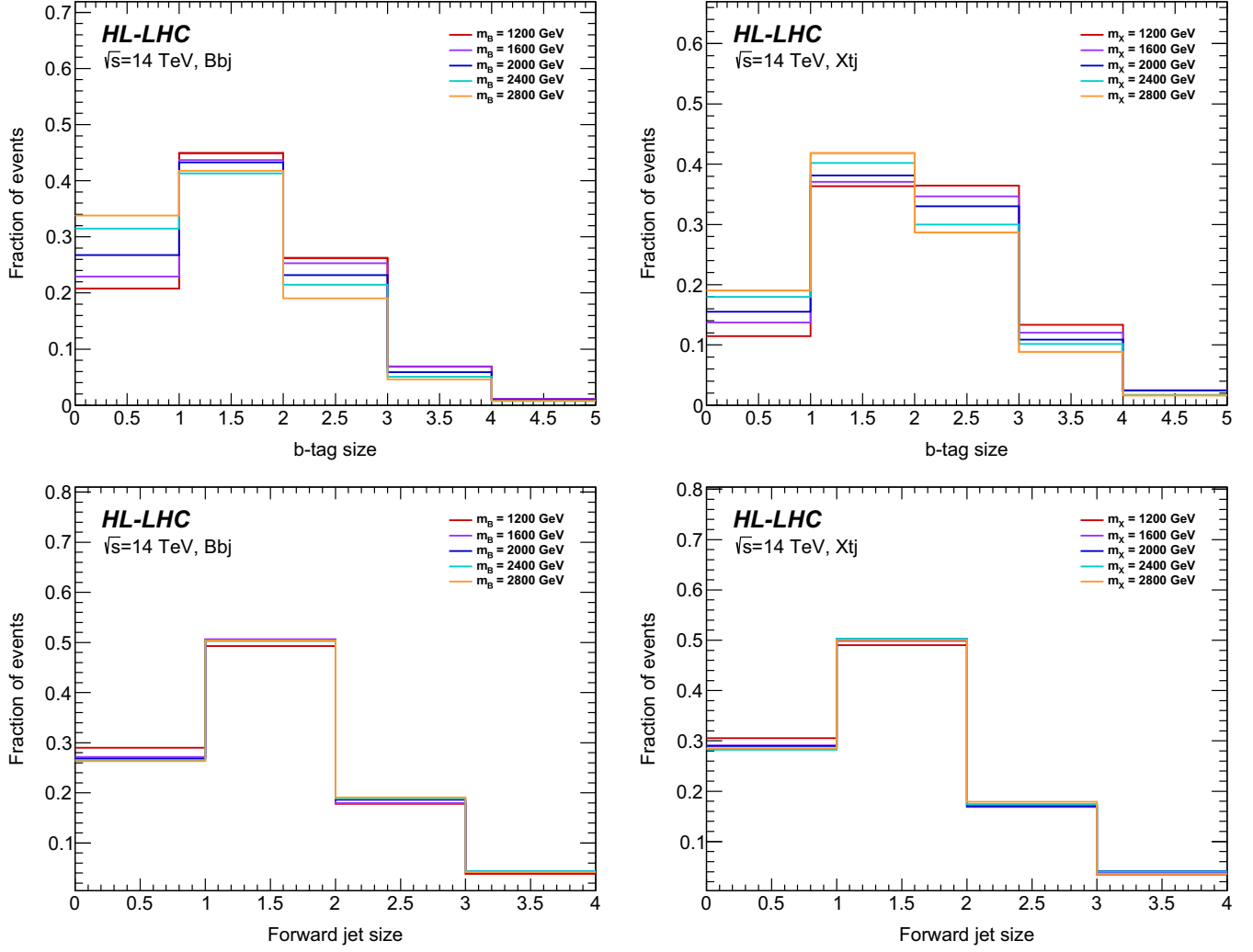


FIG. 2. The distribution of b-tag size (upper) and forward-jet size (lower) for different VLB/VLX benchmark mass values. Left (right) panels show the distributions for Bbj (Xtj) production.

generated $W + \text{jets}$ and $Z + \text{jets}$ backgrounds where a matching and merging applied.

The top quark pair production background samples are normalized to their theory predictions. The $t\bar{t}$ predicted cross section is $\sigma = 599.0$ pb, the single top predicted cross sections are $\sigma_{tj} = 0.7394$ pb, $\sigma_{tb} = 8.655$ pb, and $\sigma_{Wt} = 0.2553$ pb, which have been calculated at leading order. The event generator is used to generate $W + \text{jets}$ and $Z + \text{jets}$ events. For the $W + nj$ and $Z + nj$ modes, where $n \leq 4$, we have used $qcut = 40$ GeV value and $xqcut = 20$ GeV value for matching scheme within MadGraph5_aMC-NLO [14]. A parton jet matching scheme is employed to avoid double-counting of partonic configurations generated by both the matrix-element calculation and the parton shower [17]. These samples are generated separately for W/Z with jets. The cross section for $W + nj$ where $n \leq 4$ is calculated as $\sigma_{Wj} = 2.674 \times 10^5$ pb, and $Z + nj$ where $n \leq 4$ is calculated as $\sigma_{Zj} = 8.219 \times 10^4$ pb. Diboson events (WW , WZ , ZZ) are generated with the same event generator for the

modeling of the underlying event, which undergo further process of showering and hadronization as explained before. The corresponding cross sections for these processes are calculated as $\sigma_{WW} = 79.37$ pb, $\sigma_{WZ} = 30.21$ pb and $\sigma_{ZZ} = 11.56$ pb, respectively.

After event generation, the signal and all background samples are passed through the fast simulation of the ATLAS detector [18] based on a modular framework Delphes [19] and they are reconstructed using the procedure for the simulation data to be used in the analysis. For using the anti-kt jet algorithm [20] we have added a new FastJetFinder module within the default ATLAS card in Delphes. In this FastJetFinder module the parameter R is set to 1.0 for AK10 jets. Here, we set transverse momentum $p_T > 200$ GeV for AK10 jets.

III. EVENT SELECTION

The analysis searches for top quarks, W bosons, and b -jets to identify vector like VLB/VLX quark candidates

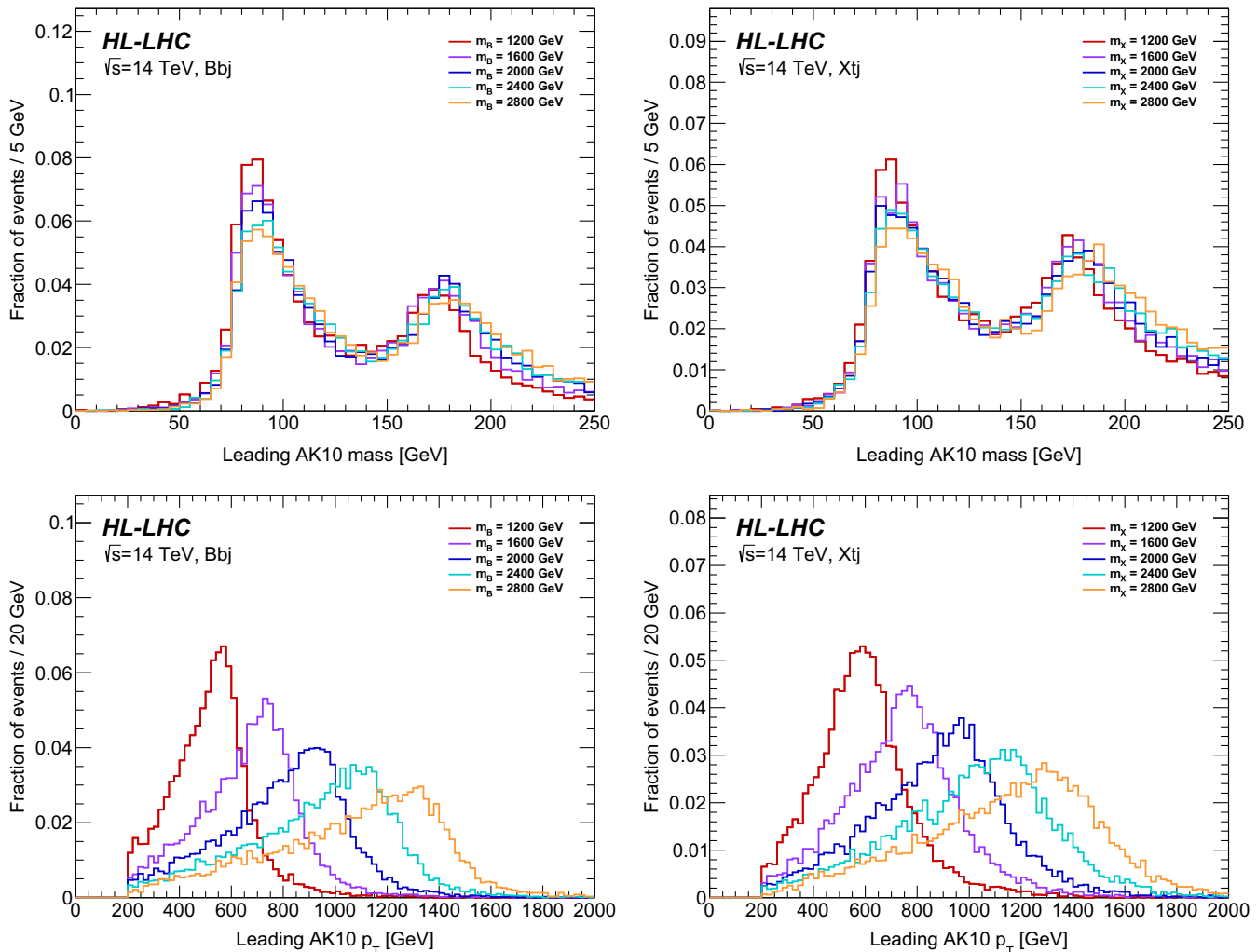


FIG. 3. The distribution of mass (upper) and transverse momentum p_T (lower) of leading AK10 jets. Left (right) panels show the distributions for Bbj (Xtj) production.

that undergo a $B/X \rightarrow Wt$ decay, followed by $t \rightarrow Wb$ and $W \rightarrow qq'$ decays. It makes use of the small-R jets (light jets), large-R jets, and event-based quantities formed from their combinations. The anti-kt algorithm [20] implemented in the FastJet package [21] is used to define two types of jets for this analysis: (1) small-R jets with $R = 0.4$ named AK4 jets, and (2) large-R jets with $R = 1.0$ named AK10 jets. These are reconstructed independently of each other, and the small-R jets use both tracking information and topological clusters [22], while the large-R jets use information from topological clusters [12] in the calorimeter.

Jet candidates are required to have $p_T > 35$ GeV in the forward region ($2.5 < |\eta| < 4.5$) and $p_T > 30$ GeV in the central region ($|\eta| < 2.5$). Jets containing b -flavored hadrons (“ b -jets”) are used to categorize the events (at least 1 b -tag jet) and reconstruct the top quark. Simulated distributions of the b -tag jet multiplicity (size) and the forward-jet size are given in Fig. 2 for the benchmark signal processes.

Each distribution has been separately normalized to unity, where the signal samples are from Bbj and Xtj processes with different VL/VLX mass values (benchmarks) ranging from $m_B = 1200$ GeV to $m_B = 2800$ GeV.

The large-R jet candidates are required to have $|\eta| < 2.0$ and $p_T > 200$ GeV in addition to their mass interval. The pseudorapidity η cut requirement is imposed to optimize the signal-to-background ratio and to select jets in a kinematic regime where the object tagging is efficient and well understood. The distribution of mass and transverse momentum p_T of leading AK10 jets is presented in Fig. 3. The p_T cut requirement ensures that the large-R jets are selected efficiently. The events are classified by using tagging states. A category for the signal are defined including top quark and W boson tagging state. The identification algorithms (“taggers”) for hadronically decaying top quarks and W bosons are utilized for the search of the VL/VLX quarks in pp collisions at HL-LHC. Distinct tagging algorithms are employed to identify these different objects.

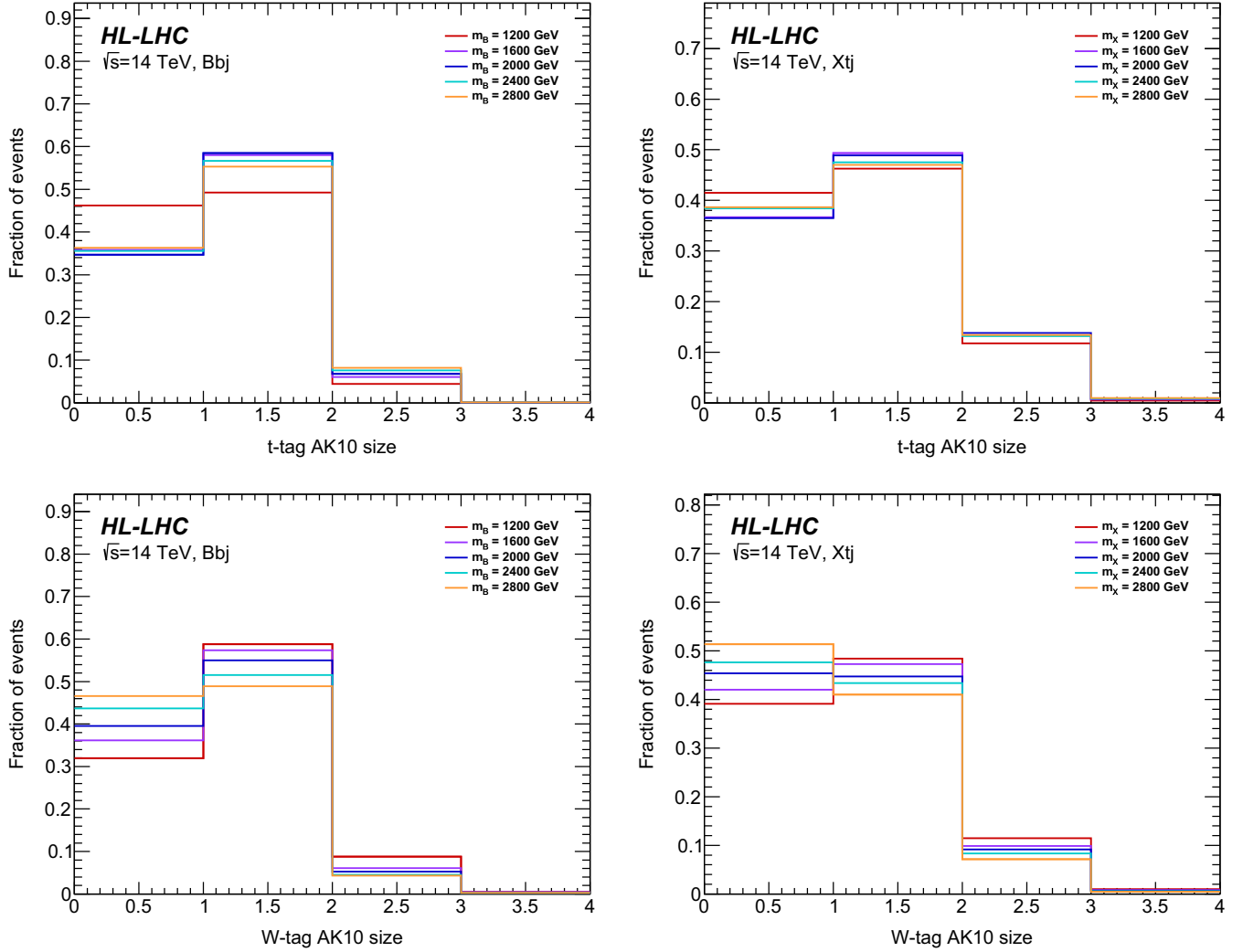


FIG. 4. The distribution of t-tag size (upper) and W-tag size (lower) for different VLX/VLB benchmark mass values. Left (right) panels show the distributions for Bbj (Xtj) production.

The top quark tagging states, consisting of quark jets which are clustered together into the AK10 jets, having $p_T > 350$ GeV and a mass between 140 and 225 GeV are considered. The W boson candidates are identified by requiring the AK10 jets, having $p_T > 200$ GeV and a mass between 60 and 105 GeV. Simulated distributions of the t-tag and W-tag multiplicity (size) are given in Fig. 4 for the benchmark signal processes.

The two highest- p_T AK10 jets are referred to as the first leading and second leading jets. All other AK10 jets are ignored. The event-tagging states are defined by the three possible tagging states of each AK10 jets as seen in Table III. In the event selection we take into account one t-tag and one W-tag state.

With these tagging definitions, the events are classified according to the tagging states of each AK10 jet: the large-R jet could be top-quark tagged, be W-boson tagged or be neither W-boson tagged nor top-quark tagged. In our case, a signal event can be in two entries in a 3×3 matrix

defined in Table III to categorize possible tagging states of the two (1st and 2nd) AK10 jets in an event. The signal region (VLX/VLB) consists of tW -tag state as illustrated with red colors in Table III. However, $2t$ -tag state or $2W$ -tag state is not considered in the signal region since we search single VLX/VLB in Wt decay channel, where one of the hadronic W boson and b-tag quark taken into account as the constituents of the top tagged events.

TABLE III. The event-tagging states defined by the tagging states of first leading and second leading AK10 jets. Relevant major backgrounds are shown in the table.

	1st AK10 jet	2nd AK10 jet	
	It	OW	Single top
	Ot	IW	W + jets
	Ot	OW	No-tag
			Ot OW
			Ot IW
			It OW
			VLB/VLX
			Dibosons
			W + jets
			Top pair
			VLB/VLX
			Single top
			It OW

TABLE IV. Summary of event selection criteria applied in the analysis.

Selection type	Value	Selection type	Value
Electron size	= 0	AK10 jet size	≥ 2
Muon size	= 0	AK10 jet $ \eta $	< 2
AK4 jet size	≥ 2	t-tagged jet p_T	> 350 [GeV]
Forward jet size	≥ 1	t-tagged jet mass interval	$140 < m_{AK10} < 225$ [GeV]
Forward jet p_T	> 35 [GeV]	W-tagged jet p_T	> 200 [GeV]
Forward jet η	> 2.5	W-tagged jet mass interval	$60 < m_{AK10} < 105$ [GeV]
b-tag size	= 1	$\Delta\phi(t, W)$	> 2
b-tag p_T	> 30 [GeV]	$\Delta R(t, b)$	< 1
b-tag $ \eta $	< 2.4	$\Delta R(W, b)$	> 2

Moreover, one of the main characteristics of the signal is the forward jet, which is benefited to separate signal from background.

For a correct reconstruction of VLX/VLB signal, we have applied topological cuts on angular separation $\Delta\phi$ and angular distance $\Delta R = \sqrt{(\Delta\eta)^2 + (\Delta\phi)^2}$. Here, we take the cut $|\Delta\phi(t, W)| > 2$ for verifying balance between the

transverse momentum of t-tag jet and W-tag jet. However, the cuts $\Delta R(t, b) < 1$ and $\Delta R(W, b) > 2$ are used to verify that b-tag jet comes from top decay.

The reconstruction of events with a t-tag and W-tag is found to be best suited for each benchmark parameter values (within high mass range) of the VLQs. The χ^2 method provide a stable performance for all VLQ masses,

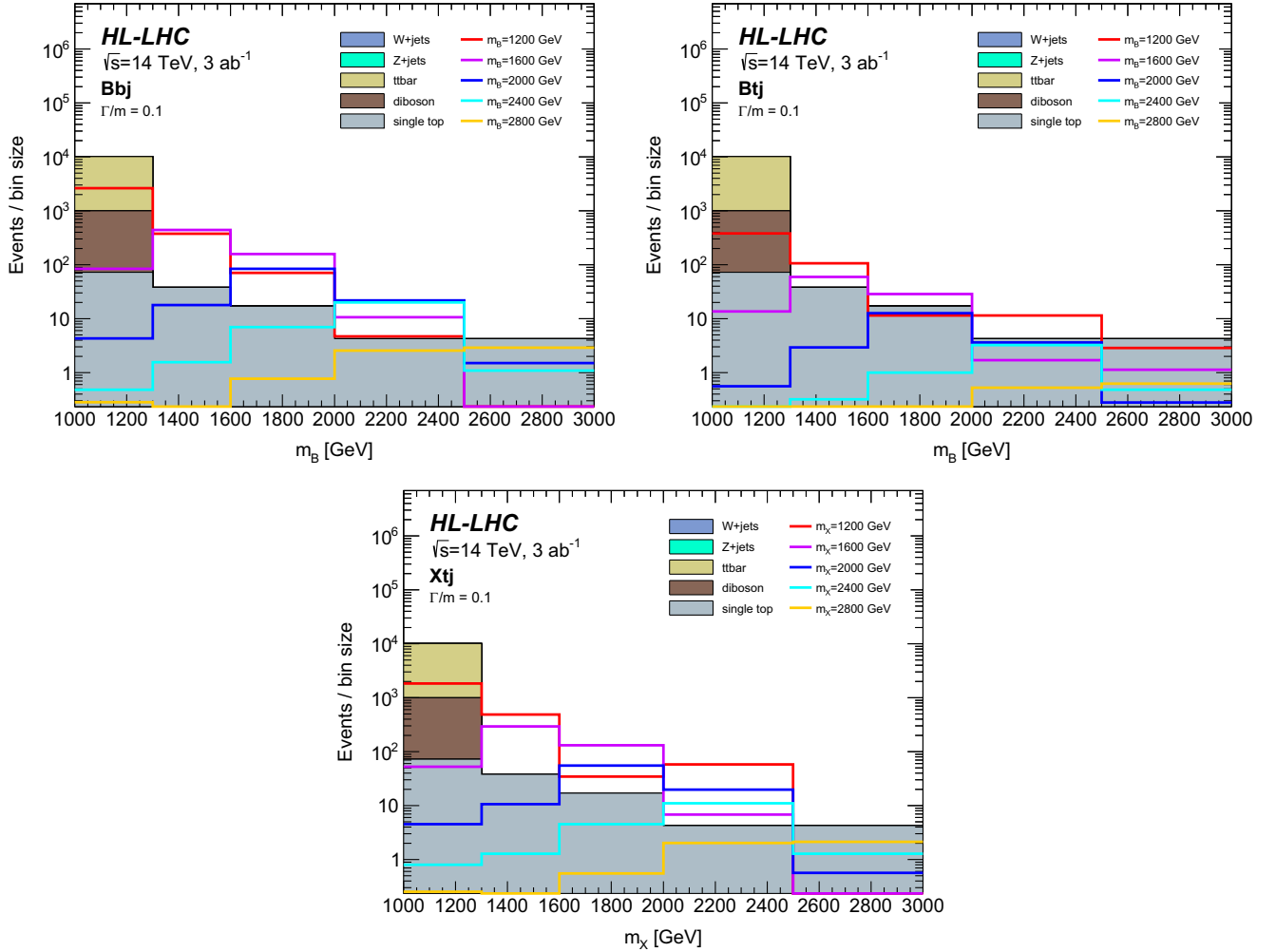


FIG. 5. Invariant mass ($m_{B/X}$) of tW system reconstructing VLB (upper: Bbj and Btj production) and VLX (lower: Xtj production) signal. The corresponding SM backgrounds are shown in stack plot.

where the VLB/VLX is reconstructed from the t-tag jet and W-tag jet.

$$\chi^2 = \frac{(\Delta R(t, W) - \pi)^2}{\sigma_{\Delta R}^2} + \frac{[(p_T^t - p_T^W)/(p_T^t + p_T^W)]^2}{\sigma_{p_T}^2}$$

For the χ^2 quantity the angular distance $\Delta R(t, W)$ and the p_T balance are used. It is verified in simulation that the expected values of $\Delta R(t, W)$ and the p_T balance are π and 0, with their standard deviations $\sigma_{\Delta R}$ and σ_{p_T} , respectively.

The main backgrounds from top pair and single top productions, W/Z + jets and Dibosons contributing backgrounds are evaluated at these categorized signal region. Together with the top quark tagged jets and W-boson tagged jets, the jets with b-tag are also included, as these typically result from mistagging a charm-quark jet arising from a CKM favored decay $W^+ \rightarrow c\bar{s}$ (or $W^- \rightarrow \bar{c}s$).

A summary of event selection criteria used in the analysis has been shown in Table IV.

IV. RECONSTRUCTION AND STATISTICS

We assume the existence of single VLB/VLX quark production in different production modes (Bbj and Btj/Xtj), the signal would appear as an excess of events with Wt invariant masses around the VLB/VLX quark mass. Reconstructed invariant mass ($m_{B/X}$) of VLB/VLX quarks is defined as $m_{B/X} = \sqrt{(p_t + p_W)^2} = \sqrt{(m_t^2 + m_W^2 + 2|\mathbf{p}_t| \cdot |\mathbf{p}_W| \cos\theta)}$. Here, the p_t and p_W are four-momentum, the \mathbf{p}_t and \mathbf{p}_W are momentum vectors of top quark and W-boson, respectively. The most probable value for the $\cos\theta$ can be set, since these two objects are mostly back to back, because of the heavy object resonant production. However, in the analysis of signal and background samples we use the physics four-vectors within the Root 6 [23], and the analysis code has been developed using PYTHON interface PyRoot which is able to interoperate with widely-used PYTHON data-science libraries.

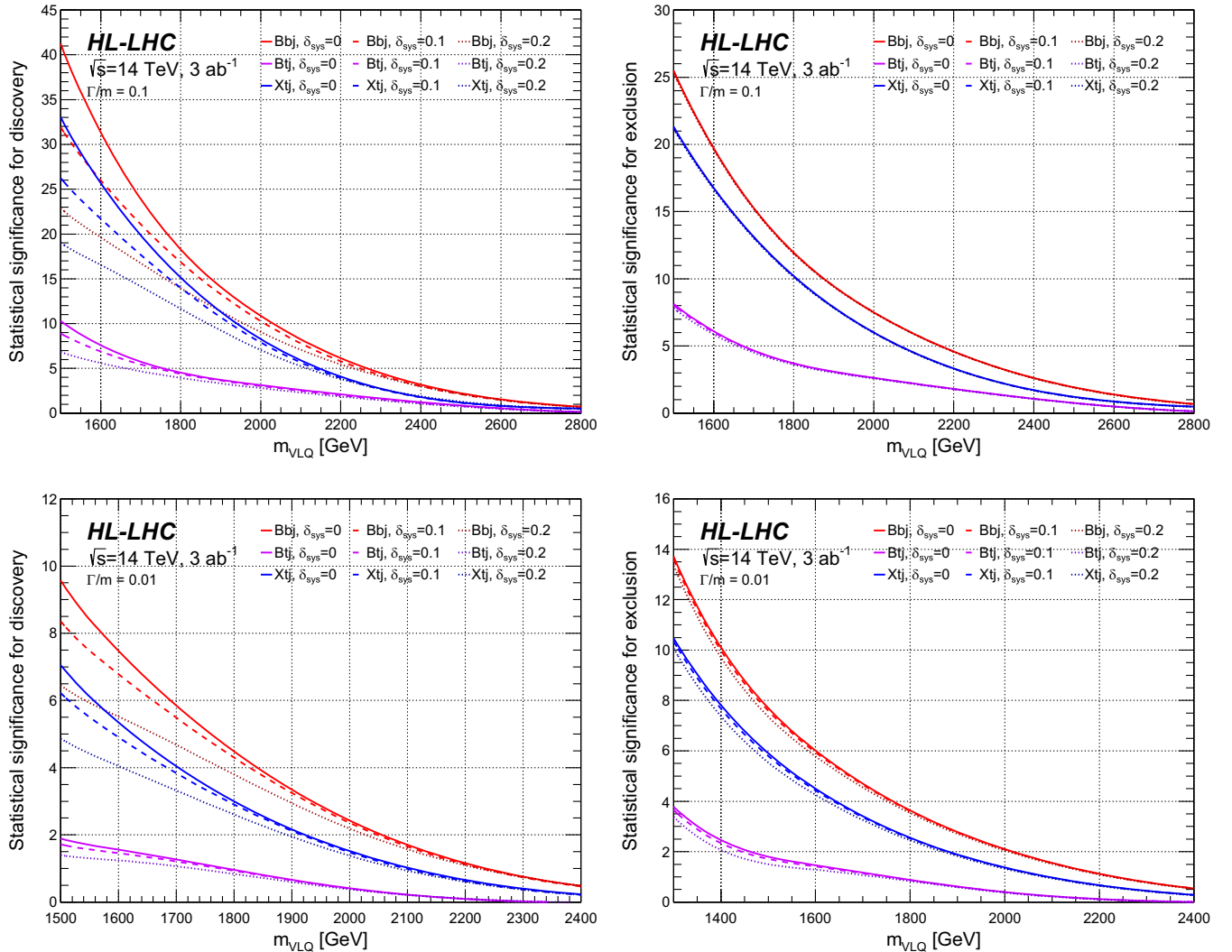


FIG. 6. Significance for the discovery (left) and exclusion (right) of VLB/VLX signal for the production process Bbj and Btj/Xtj .

The reconstructed mass distributions for the signal category is presented in Fig. 5. In the figure, the left panel shows Bbj production mode, while right panel shows the production mode Xtj . From the invariant mass distributions for Bbj and Btj/Xtj processes the number of

expected events for signal and background have been calculated in the mass window 10% of the VLB/VLX mass values.

In order to analyze the sensitivity, we use the statistical significance (SS) for expected discovery (SS_{dis}) limits [24]

$$SS_{\text{dis}} = \sqrt{2 \left[(S+B) \ln \left(\frac{(S+B)(1+\delta_{\text{sys}}^2 B)}{B+(S+B)\delta_{\text{sys}}^2 B} \right) - \frac{1}{\delta_{\text{sys}}^2} \ln \left(1 + \frac{\delta_{\text{sys}}^2 S}{1+\delta_{\text{sys}}^2 B} \right) \right]}$$

and exclusion (SS_{exc}) limits

$$SS_{\text{exc}} = \sqrt{2 \left[S - B \ln \left(\frac{(S+B+X)}{2B} \right) - \frac{1}{\delta_{\text{sys}}^2} \ln \left(\frac{B-S+X}{2B} \right) \right] - (B+S-X) \left(1 + \frac{1}{\delta_{\text{sys}}^2 B} \right)}$$

with

$$X = \sqrt{(S+B)^2 - 4S\delta_{\text{sys}}^2 B^2 / (1 + \delta_{\text{sys}}^2 B)}$$

Here, S and B are the expected number of events for the signal and background, respectively. These can be obtained by multiplying the production cross sections, branchings and the integrated luminosity together with the corresponding efficiencies for interested search channel. The systematic uncertainty (δ_{sys} in percentage) on the estimated SM background is already included in the significance. However, in the limit case ($\delta_{\text{sys}} \rightarrow 0$) we obtain these expressions as $SS_{\text{dis}} = \sqrt{2[(S+B) \ln(1+S/B) - S]}$ and $SS_{\text{exc}} = \sqrt{2[S - B \ln(1+S/B)]}$ as already used in many of the phenomenological studies.

As a result, in Fig. 6, we present exclusion plot and discovery plot with three different systematic uncertainty cases: no systematics ($\delta_{\text{sys}} \rightarrow 0$), a mild systematic of $\delta_{\text{sys}} = 10\%$, and an possible systematic of $\delta_{\text{sys}} = 20\%$. The mass limits from the discovery plot is effected by the systematic uncertainties. One can see that with a possible uncertainty of 20%, sensitivities are slightly weaker than those with a mild systematic uncertainty of 10%. For a width to mass ratio of $\Gamma_{B/X}/M_{B/X} = 0.1$, the VLB (VLX) can be discovered (with 5σ level) with a mass about 2273 (2145) GeV at HL-LHC with an integrated luminosity of 3 ab^{-1} . Out of a discovery, one can also set 95% C.L. exclusion limits 2491 (2364) GeV on the mass of VLB (VLX) for the same integrated luminosity. For more narrow width case as $\Gamma_{B/X}/M_{B/X} = 0.01$, the VLB (VLX) can be discovered (with 5σ level) with a mass about 1764 (1618) GeV at HL-LHC with an integrated luminosity of 3 ab^{-1} . Out of a discovery, one can also set 95% C.L. exclusion limits 2018 (1873) GeV on the mass

of VLB (VLX) for the same integrated luminosity. Mass limits on VLB/VLX for three different production processes and systematic uncertainty cases are shown in Table V. For a comparison with other case corresponding to $\Gamma_{B/X}/M_{B/X} = 0.01$, we present accessible discovery and exclusion mass limits on VLB/VLX for different production processes and systematic uncertainty cases are shown in Table VI.

TABLE V. Mass limit for evidence (3σ) / discovery (5σ) and exclusion (2σ) of VLB/VLX signal at the HL-LHC with $L_{\text{int}} = 3 \text{ ab}^{-1}$. Here, the relative width is taken as $\Gamma_{B/X}/m_{B/X} = 0.1$. Each panel corresponds to different systematic uncertainty case, denoting no systematics, a mild systematic case $\delta_{\text{sys}} = 10\%$ and a possible systematic case $\delta_{\text{sys}} = 20\%$.

Process	Mass Limits [GeV]	
	Evidence (3σ)/Discovery (5σ)	Exclusion (2σ)
$\delta_{\text{sys}} = 0$		
Bbj	2418/2273	2491
Btj	2018/1764	2145
Xtj	2273/2145	2364
$\delta_{\text{sys}} = 10\%$		
Bbj	2344/2163	2490
Btj	1909/1672	2144
Xtj	2235/2055	2345
$\delta_{\text{sys}} = 20\%$		
Bbj	2400/2236	2490
Btj	1964/1655	2144
Xtj	2273/2109	2344

TABLE VI. The same as Table V, but for relative width $\Gamma_{B/X}/m_{B/X} = 0.01$.

Process			Mass Limits [GeV]		
$\delta_{\text{sys}} = 0$	Evidence (3σ)/Discovery (5σ)		Exclusion (2σ)		
Bbj	1927/1764		2018		
Btj	1382/1273		1455		
Xtj	1800/1618		1873		
$\delta_{\text{sys}} = 10\%$					
Bbj	1926/1745		2017		
Btj	1345/1255		1436		
Xtj	1782/1600		1872		
$\delta_{\text{sys}} = 20\%$					
Bbj	1891/1655		2000		
Btj	1309/1218		1400		
Xtj	1745/1491		1872		

V. CONCLUSIONS

We have investigated single production of the VLB/VLX quarks in the 4FNS scheme at 14 TeV HL-LHC via the process $pp \rightarrow Bbj$ and $pp \rightarrow Btj/Xtj$ with a subsequent decay channel $B \rightarrow Wt(t \rightarrow Wb)$ (where the W bosons decay hadronically $W \rightarrow jj$) in a simplified model framework of vectorlike quarks B/X, where only two parameters are contained in one type of VLQs, the VLB/VLX quark mass $m_{B/X}$ and the decay width-to-mass ratio ($\Gamma_{B/X}/m_{B/X}$). Then, our study is relevant to the VLB in one of the singlet (B), doublet (TB) or triplet (TBY) branching scenarios for the Bbj and Btj production, while it is relevant to the VLX

in one of the doublet (XT) or triplet (XTB) scenarios for the Xtj production. We have performed a fast detector simulation for the signal and the relevant SM backgrounds. This search presents a significant advance over previous searches for VLB/VLX searches at the pp collisions. We present our results showing that, with an integrated luminosity of 3 ab^{-1} at the HL-LHC, the discovery range can reach the VLB (VLX) mass up to 2273(2145) GeV without considering the systematic uncertainty. When a possible systematic uncertainty of 20% is included, we find an accessible range of mass up to 2236(2109) GeV, respectively. On the other hand, the 95% C.L. exclusion limits for the masses up to 2490(2344) GeV for VLB(VLX), in the case of a possible systematic uncertainty of $\delta_{\text{sys}} = 20\%$. We see that the excluding capabilities (a similar interpretation for the discovery capability) of VLB/VLX searches are enhanced with the increase of both the center-of-mass energy and integrated luminosity of HL-LHC. We expect our study can be guideline search for a possible VLB/VLX quark at the future pp colliders.

ACKNOWLEDGMENTS

We would like to thank Ankara University High Energy Physics (AUHEP) group for fruitful discussions. The numerical calculations reported in this paper were partially performed at TUBITAK ULAKBIM, High Performance and Grid Computing Center (TRUBA resources). The work was supported in part by the Turkish Energy, Nuclear and Mineral Research Agency (TENMAK) under project Grant No. 2020TAEK(CERN)A5.H1.F5-25.

-
- [1] ATLAS Collaboration, Measurement of the cross section for producing a W boson in association with a single top quark in pp collisions at $\sqrt{s} = 13$ TeV with ATLAS, *J. High Energy Phys.* **01** (2018) 063; Measurement of differential cross sections of a single top quark produced in association with a W boson at $\sqrt{s} = 13$ TeV with ATLAS, *Eur. Phys. J. C* **78**, 186 (2018).
 - [2] CMS Collaboration, Measurement of the production cross section for single top quarks in association with W bosons in proton-proton collisions at $\sqrt{s} = 13$ TeV, *J. High Energy Phys.* **10** (2018) 117.
 - [3] J. A. Aguilar-Saavedra, Identifying top partners at LHC, *J. High Energy Phys.* **11** (2009) 030.
 - [4] N. Vignaroli, Early discovery of top partners and test of the Higgs nature, *Phys. Rev. D* **86**, 075017 (2012).
 - [5] J. A. Aguilar-Saavedra, Mixing with vectorlike quarks: Constraints and expectations, *EPJ Web Conf.* **60**, 16012 (2013).
 - [6] J. A. Aguilar-Saavedra, R. Benbrik, S. Heinemeyer, and M. Perez-Victoria, Handbook of vectorlike quarks: Mixing and single production, *Phys. Rev. D* **88**, 094010 (2013).
 - [7] J. M. Alves *et al.*, Vectorlike singlet quarks: A roadmap, [arXiv:2304.10561v2](https://arxiv.org/abs/2304.10561v2).
 - [8] G. Aad *et al.* (The ATLAS Collaboration), Search for the production of single vectorlike and excited quarks in the Wt final state in pp collisions at $\sqrt{s} = 8$ TeV with the ATLAS detector, *J. High Energy Phys.* **02** (2016) 110.
 - [9] A. M. Sirunyan *et al.* (CMS Collaboration), Search for single production of vector-like quarks decaying to a b quark and a Higgs boson, *J. High Energy Phys.* **06** (2018) 031.
 - [10] A. M. Sirunyan *et al.* (The CMS Collaboration), Search for single production of vector-like quarks decaying to a top quark and a W boson in proton-proton collisions at $\sqrt{s} = 13$ TeV, *Eur. Phys. J. C* **79**, 90 (2019).

- [11] G. Aad *et al.* (ATLAS Collaboration), Search for single vector-like B quark production and decay via $B \rightarrow bH(\bar{b}b)$ in pp collisions at $\sqrt{s} = 13$ TeV with the ATLAS detector, Report No. ATLAS-CONF-2021-018, 2021.
- [12] ATLAS Collaboration, Performance of top-quark and W -boson tagging with ATLAS in run 2 of the LHC, *Eur. Phys. J. C* **79**, 375 (2019).
- [13] Benjamin Fuks and Hua-Sheng Shao, QCD next-to-leading-order predictions matched to parton showers for vector-like quark models, *Eur. Phys. J. C* **77**, 135 (2017).
- [14] J. Alwall, R. Frederix, S. Frixione, V. Hirschi, F. Maltoni, O. Mattelaer, H.-S. Shao, T. Stelzer, P. Torrielli, and M. Zaro, The automated computation of tree-level and next-to-leading order differential cross sections, and their matching to parton shower simulations, *J. High Energy Phys.* **07** (2014) 079.
- [15] R. D. Ball, V. Bertone, S. Carazza, C. S. Deans, L. D. Debbio, S. Forte, A. Guffanti, N. P. Hartland, J. I. Latorre, J. Rojo, and M. Ubiali (The NNPDF collaboration), Parton distributions for the LHC run II, *J. High Energy Phys.* **04** (2015) 040.
- [16] T. Sjöstrand, S. Ask, J. R. Christiansen, R. Corke, N. Desai, P. Ilten, S. Mrenna, S. Prestel, C. O. Rasmussen, and P. Z. Skands, An introduction to PYTHIA 8.2, *Comput. Phys. Commun.* **191**, 159 (2015); T. Sjöstrand, The pythia event generator: Past, present and future, *Comput. Phys. Commun.* **246**, 106910 (2020).
- [17] M. L. Mangano, M. Moretti, and R. Pittau, Multijet matrix elements and shower evolution in hadronic collisions: $Wb\bar{b} + n$ jets as a case study, *Nucl. Phys.* **B632**, 343 (2002); S. Hoeche, F. Krauss, N. Lavesson, L. Lonnblad, M. Mangano, A. Schalicke, and S. Schumann, Matching parton showers and matrix elements, [arXiv:hep-ph/0602031](https://arxiv.org/abs/hep-ph/0602031).
- [18] ATLAS Collaboration, The ATLAS experiment at the CERN Large Hadron Collider, *J. Instrum.* **3**, S08003 (2008).
- [19] J. de Favereau, C. Delaere, P. Demin, A. Giammanco, V. Lemaître, A. Mertens, and M. Selvaggi (The DELPHES 3 Collaboration), DELPHES 3: A modular framework for fast simulation of a generic collider experiment, *J. High Energy Phys.* **02** (2014) 057.
- [20] Matteo Cacciari, Gavin P. Salam, and Gregory Soyez, The anti- k_t jet clustering algorithm, *J. High Energy Phys.* **04** (2008) 063.
- [21] M. Cacciari, G. P. Salam, and G. Soyez, Fastjet user manual, *Eur. Phys. J. C* **72**, 1896 (2012).
- [22] ATLAS Collaboration, Jet reconstruction and performance using particle flow with the ATLAS Detector, *Eur. Phys. J. C* **77**, 466 (2017).
- [23] Rene Brun and Fons Rademakers, ROOT—An object oriented data analysis framework, *Nucl. Instrum. Methods Phys. Res., Sect. A* **389**, 81 (1997).
- [24] Glen Cowan, Kyle Cranmer, Eilam Gross, and Ofer Vitells, Asymptotic formulae for likelihood-based tests of new physics, *Eur. Phys. J. C* **71**, 1554 (2011).